NASA SP-330

APOLLO 17

Preliminary Science Report

PREPARED BY

LYNDON B. JOHNSON SPACE CENTER

Scientific and Technical Information Office 1973

NATIONAL AERONAUTICS AND SPACE ADMINISTRATION

Washington, D.C.

16. Lunar Ejecta and Meteorites Experiment

O. E. Berg,[a†] *F. F. Richardson,*[a] *and H. Burton*[a]

For the past 20 yr, astronomical interest in the cosmic dust particle has been partially dominated by a concern for the mechanical devastation imparted by meteoroid impacts or the so-called meteoroid hazard. Today, the meteoroid hazard has been accurately evaluated and found to be essentially nonexistent (ref. 16-1). Now we are witnessing an interesting period of transition for cosmic dust studies from simply determining the number and size of particles impinging on a certain area in a certain time to an astronomical interest in the nature and the source of the material. The cosmic dust particle is emerging as a much more interesting object than its larger cousin, the meteoroid, which is often seen blazing a path across the atmosphere of the Earth. Both are affected by gravity, solar wind erosion, and planetary atmospheres, but, because of its small size and consequently its high surface-to-mass ratio, the micrometeoroid is also significantly affected by solar radiation pressure, magnetic fields, electric fields, and probably the shadow or umbra of the Earth. The extraterrestrial microparticles encountered by the lunar ejecta and meteorites (LEAM) experiment may be divided into three distinct and interesting classes: lunar ejecta, interstellar grains, and cometary debris.

OBJECTIVES

The lunar ejecta particle depicted in figure 16-1 is the offspring of a meteoroid encounter with the lunar surface. The Moon, like the Earth, is continually bombarded by meteoroids traveling at hypervelocities (speeds in excess of the speed of sound in a material (ref. 16-2)). The lunar surface, unprotected by an atmosphere, receives the impact at full velocity from 2.4 to 72 km/sec. Because of the high velocity, the projectile and the immediate area of the impact become molten and behave similarly to liquid masses. Secondary particles (or lunar ejecta) are ejected radially and at high velocities from the impact site. The volume of lunar ejecta material relative to primary particle volume and the range of velocities for lunar ejecta are currently conjecture based on laboratory studies using hypervelocity projectiles. Lunar ejecta mass is probably comparable, in most cases, to the mass of the impacting meteoroid. Laboratory studies have shown that ejecta velocities may exceed the primary particle velocity, but, in general, it is assumed that a relatively small percentage of the ejecta particles have velocities in excess of the lunar escape velocity of 2.4 km/sec; thus, the bulk of material returns to the lunar surface (ref. 16-3). The LEAM experiment intercepts ejecta particles and records information useful in establishing the history of the Moon.

The manner in which interstellar particles or grains invade our solar system is depicted in figure 16-2. Our

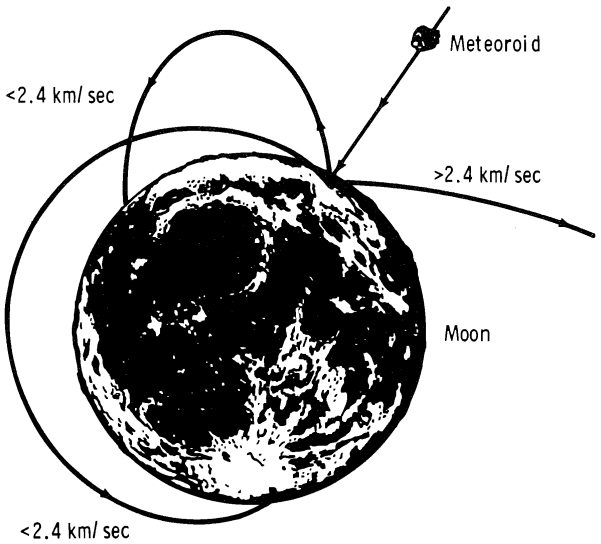

FIGURE 16-1.–Lunar ejecta.

[a]NASA Goddard Space Flight Center.
[†]Principal Investigator.

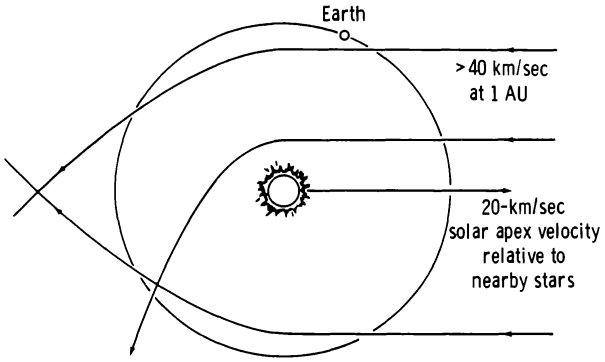

FIGURE 16-2.–Interstellar grains. Interstellar grains <40 km/sec are trapped by the solar system; those >40 km/sec pass on through.

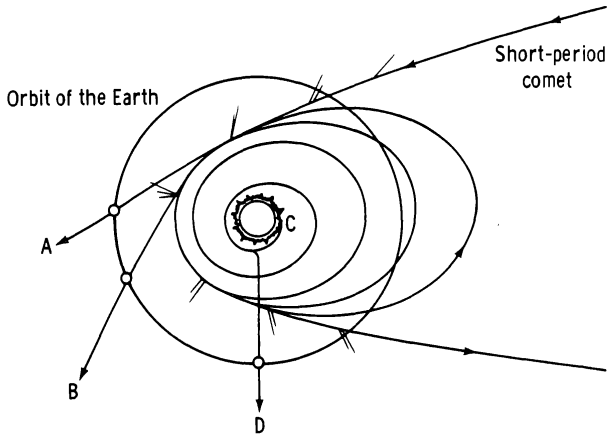

FIGURE 16-3.–Cometary debris.

Sun and its planets are moving through the Milky Way Galaxy at approximately 20 km/sec relative to nearby stars. In so doing, our solar system passes through "clouds" of interstellar dust (ref. 16-4) with relative encounter velocities approaching and possibly exceeding 100 km/sec. Although the particles are extremely small (probably 10^{-15} g), their detection probability by the LEAM experiment is high because the experiment responds to the cube of the particle velocity; thus, it is extremely sensitive to high-speed particles. Two forerunners of the LEAM experiment, in the heliocentric satellites Pioneer 8 and 9, have detected two (and possibly more) interstellar grains that are believed to be the first impact registrations of this type of particle (ref. 16-5). Because the LEAM experiment measures particle speed, radiant (or source) direction, and particle kinetic energy, the encounters by interstellar grains may be readily distinguished from encounters by other types of cosmic dust.

Cometary debris is considered the most abundant component of cosmic dust within our solar system. It is generally accepted that comets are gigantic "dirty snowballs" with nuclei diameters on the order of 10 km and are principally composed of frozen mixtures of gases and liquids (ref. 16-6). Embedded in this "snowball" are solids ranging in diameters from tenths of micrometers to large boulders. As the comet approaches its perihelion, as shown in figure 16-3, it undergoes partial disintegration because of the effects of radiation pressure and spews out a tail of gases, vapors, and solid particulates. For larger comets, the tail is often visible to the eye as diffuse illumination pointing away from the Sun. Large particulate matter may separate from the parent comet and attain a heliocentric orbit similar to its parent; the large particulates will remain in this orbit until they are perturbed by other planets or bodies or collide with the Moon, the Earth, or other planets. These large particulates are the blazing meteoroids mentioned previously. After separation from the parent comet, the smaller particulates, micrometeoroids, behave much less predictably because they are affected by two forces: the force of gravity, which is a function of the particle mass and therefore the cube of the particle radius ($4/3\pi r^3$) and the force of solar radiation pressure, which is a function of the cross-sectional area of the particle and therefore the square of the radius (πr^2). If the force of radiation pressure exceeds the force of gravity at the moment of separation from the parent comet, the particle will assume a hyperbolic trajectory, as shown for *A* and *B* in figure 16-3, and the particle will leave our solar system. If the force of gravity exceeds the force of radiation pressure at the moment of separation from the parent comet, the particle will spiral in toward the Sun very slowly under the Poynting-Robertson effect. Here again, as postulated, a second separation of particles occurs (ref. 16-7). Because of their heat capacity, the larger dust particles continue into the Sun and are absorbed, as shown by *C*. As the smaller dust particles approach to within a few solar radii of the Sun, they partially evaporate, and, because the relative mass or gravity (r^3) reduction is faster than the relative cross-sectional area (r^2) reduction, the force of radiation pressure soon exceeds the force of gravity for the particle, and it is ejected quasi-radially from the Sun, as depicted by *D*.

Essentially all the particles intercepted by the Pioneer 8 and 9 instruments were outgoing particles,

suggesting ejected cometary fragments rather than particles in elliptical orbits (ref. 16-8). Accordingly, the LEAM experiment is shielded by the Moon from primary particle impacts during lunar night. However, the formation and presence of lunar ejecta from large meteoroid impacts are quite independent of lunar day/night conditions—a set of conditions that helps to distinguish between impacts by primary particle events and impacts by lunar ejecta. During each lunar cycle, each of three sensor systems incorporated into the LEAM experiment is alternately exposed to and shielded from impacts by these particles.

The position of the LEAM experiment on the lunar surface and the associated alternated exposure and shielding feature of the sensor systems offer an opportunity for the experiment to verify Earth focusing effects (fig. 16-4). Microparticles that are ejected, one way or another, into our solar system will tend to be ejected radially away from the Sun. For simplicity, microparticles are shown as having parallel trajectories in figure 16-4. As they are blown past the Earth, they are perturbed toward the Earth and tend to focus into a concentration extending outward from the shaded side of the Earth. Thus, as shown in figure 16-4, the LEAM experiment will, once per lunar cycle, be ideally exposed to this postulated concentration and/or perturbation effects.

THE LEAM INSTRUMENT

The major objectives of placing a cosmic dust experiment on the Moon can readily be met by the LEAM instrument (fig. 16-5). This instrument measures the particle speed, particle direction, total particle energy (kinetic), and particle momentum for particles having parameters as shown. The LEAM

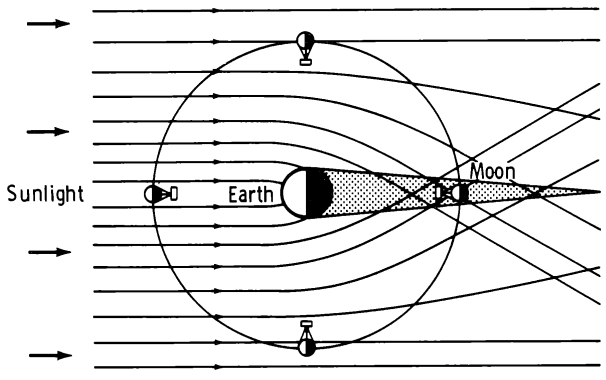

FIGURE 16-4.–Earth focusing effect.

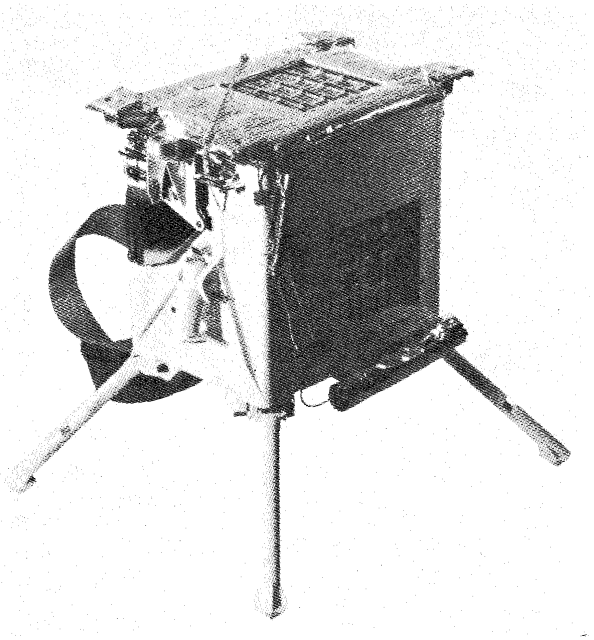

FIGURE 16-5.–The LEAM experiment, which responds to impacts of microparticles having a mass as low as 10^{-14} g, a diameter as small as 2×10^{-5} cm, and a speed as high as 75 km/sec.

experiment consists of three sensor systems: the east sensor, the west sensor, and the up sensor. Only the up and west sensors are visible in figure 16-5.

The basic sensor for each array is shown schematically in figure 16-6. The basic sensor consists of a front (A) film-grid sensor array and a rear (B) film-grid sensor array spaced 5 cm apart (film plane to film plane) and an acoustical impact plate upon which the rear film is mounted. The performance of the sensors depends upon two basic measurable phenomena that occur when a hypervelocity particle impacts upon a surface: the formation of a plasma and a transfer of momentum.

In conjunction with the following explanation of the operation of the LEAM experiment, refer to figure 16-6 and consider three probable types of cosmic dust particles: a high-energy hypervelocity particle (>1.0 erg); a low-energy hypervelocity particle (<1.0 erg); and a relatively large high-velocity particle ($>10^{-10}$ g). The third type includes the majority of lunar ejecta particles. As a high-energy hypervelocity particle enters the front film sensor, it yields some of its kinetic energy toward the generation of ionized plasma at the front film. Electrons from the plasma are collected on the positively biased grid (+24 V), producing a negative-going pulse that is

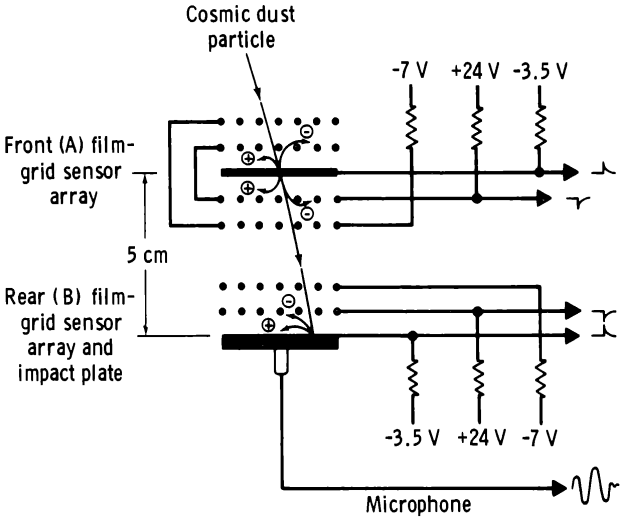

FIGURE 16-6.–The basic sensor.

amplified as shown (fig. 16-6). The ions from the plasma are collected on the negatively biased film (–3.5 V), producing a positive-going pulse that is amplified as shown (fig. 16-6) and pulse-height-analyzed as a measure of the kinetic energy of the particle. As the particle continues on its path, it yields its remaining energy at the rear sensor film (and plate), generating a second set of plasma pulses and an acoustical pulse (if the momentum of the particle is sufficient). A pulse-height analysis is performed on the positive-going plasma pulse, and a peak-pulse-height analysis is performed on the acoustical sensor output as a measure of the remaining momentum of the particle.

As a low-energy hypervelocity particle enters the front sensor, it yields all its kinetic energy at the front film. A pulse-height analysis is performed on the positive output signal as a measure of the kinetic energy of the particle.

As a relatively large high-velocity particle enters the LEAM experiment, it may pass through the front and rear film sensor arrays without generating a detectable ionized plasma but still impart a measurable impulse to the acoustical sensor. In this event, a peak-pulse-height analysis is performed on the acoustical sensor output pulse.

An electronic clock registers the time of flight of the particle as the time lapse between positive pulses (front film and rear film output signals), which is used to derive the speed of the particle. The time-of-flight sensor represents one of 256 similar sensor systems that comprise the east and up sensor arrays. The west sensor array was designed specifically to record low-speed ejecta impacts on the microphone plate without retardation by a front film; consequently, this array has no capability to measure particle speed. Figure 16-7, an exploded schematic of the overall LEAM experiment, shows that four vertical film strips are crossed by four horizontal grid strips to affect 16 front and 16 rear film sensor arrays, creating 256 possible combinations. Each grid strip and each film strip connects to a separate output amplifier. The output signals from these amplifiers are used to determine the segment in which an impact occurred. Thus, knowing what front film segment was penetrated and what rear film segment was affected by an impact, the direction of the incoming particle can be determined with respect to the sensor axis and, eventually, to the Sun.

SENSOR CONTROLS

An ideal sensor control is one that is exposed to the same environment as the active or main sensor. Environment encompasses electrical and magnetic radiation, thermal radiation, thermal gradients, and so forth. Controls installed somewhere in the experiment and sheltered from the total environment are ineffective. The controls used in this experiment are designed to perform, as much as possible, under the same conditions as the main sensor. An upper portion of the rear film array and a lower portion of the front film array of the east sensor system are used as controls for the plasma sensors. An epoxy resin coating covers the control grids and films, isolating them from the products of ionization caused by impacts on their area (e.g., electrons and ions generated by hypervelocity impacts on the epoxy cannot be collected on the grids or films). However, the resin coat does not constitute a shield from electrical or magnetic radiation. (Thermal noise is not an important factor in ionization sensors.) A microphone control is unique in that it is a "live microphone" attached to a separate impact plate having one-third the effective area of the main microphone plate. Thus, the control is truly exposed to the same environment as the main microphone sensor, including impacts by cosmic dust; an approximate ratio of 1:3 would be expected between impacts on the control and impacts on the main microphone sensor.

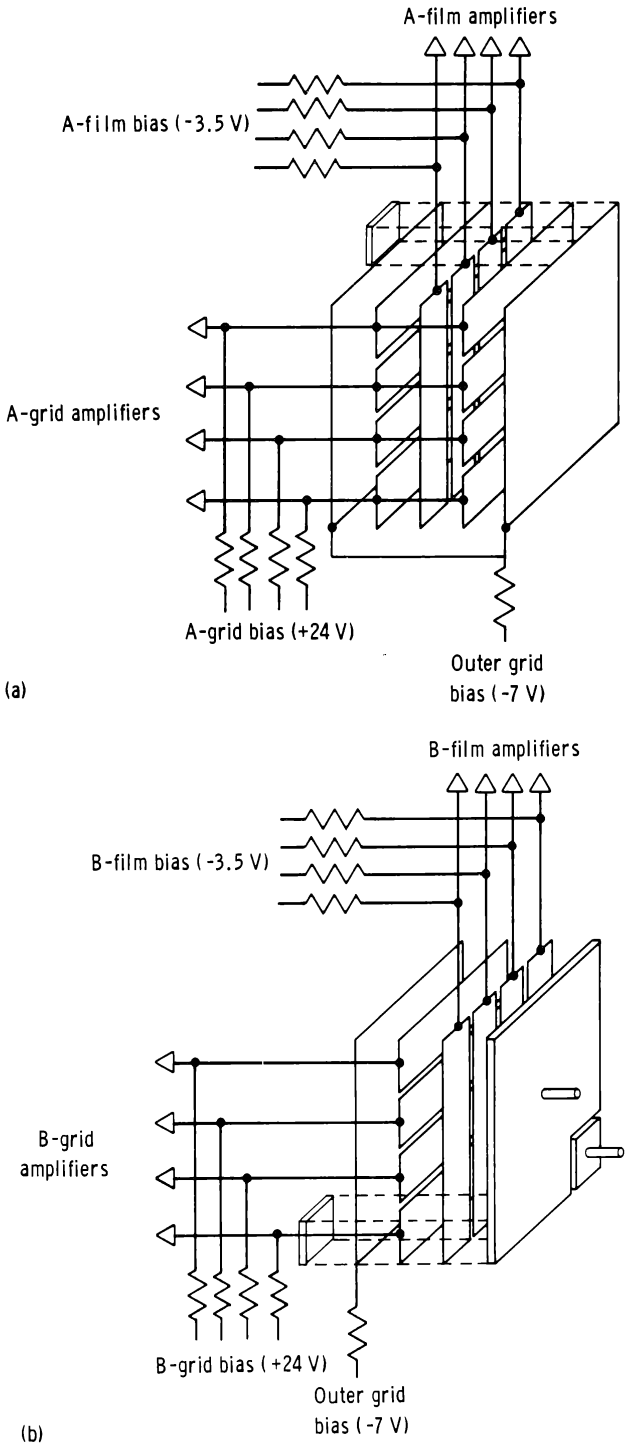

FIGURE 16-7.—Schematic of time-of-flight sensor. (a) Front sensor array. (b) Rear sensor array.

CALIBRATIONS

Extensive calibrations have been performed on the sensors using a 2-MV electrostatic accelerator. Unfortunately, the particles used for calibration have been limited to high-density hard spheres of iron (10^{-13} g < mass < 10^{-9} g) and to velocities corresponding to the low end of the meteoroid velocity spectrum (1 to 25 km/sec). Accordingly, when considering the sensitivities of the sensors as derived from these calibrations, the possible latent discrepancies must be considered that may become manifest in subsequent measurements in space when the sensors are exposed to projectiles of diverse density, structure, composition, and higher velocities. The plasma sensors respond nearly linearly to the product $mv^{2.6}$ (m = mass, v = velocity) over the limited particle parameter range specified previously for the laboratory simulator. The acoustical sensors respond to the momentum of the particle for that same particle range. The threshold sensitivity of the front film sensor array to laboratory particles is 0.6 erg. Time of flight is registered for laboratory particles having kinetic energies of 1.0 erg or greater. The electronics of the time-of-flight sensor are design limited to particles having velocities ranging from 2 to 72 km/sec. The threshold sensitivity of the acoustical sensor is 2×10^{-5} dyn-sec (including deceleration by the front film).

Hypervelocity particles passing through the front film of the sensors are decelerated in inverse proportion to their kinetic energy (for a velocity range of 1 to 20 km/sec). For particles having the minimum energy required to exhibit time of flight (1.0 erg), the deceleration is 40 percent. Deceleration drops to 5 percent for particles having 10 ergs. In situ calibration is provided and can be initiated either automatically or by ground command. Two different formats of simulated data pulses are alternately presented by the experiment to the input of each of the amplifier systems to check the condition of the electronics and the plasma sensors. Two formats alternately provide a high and a low amplitude pulse to monitor the lower and the upper sensitivities of the amplifiers. Front film sensor pulses and rear film sensor pulses are appropriately spaced and in proper sequence to monitor the time-of-flight electronics. All accumulators advance with inflight calibration.

EXPERIMENT ELECTRONICS

A simple block diagram of the electronics in one of the dual (east, up) sensor arrays is shown in figure 16-8. A preamplifier receives the positive-going pulse from each A-film strip. After a gain of 3, the pulse

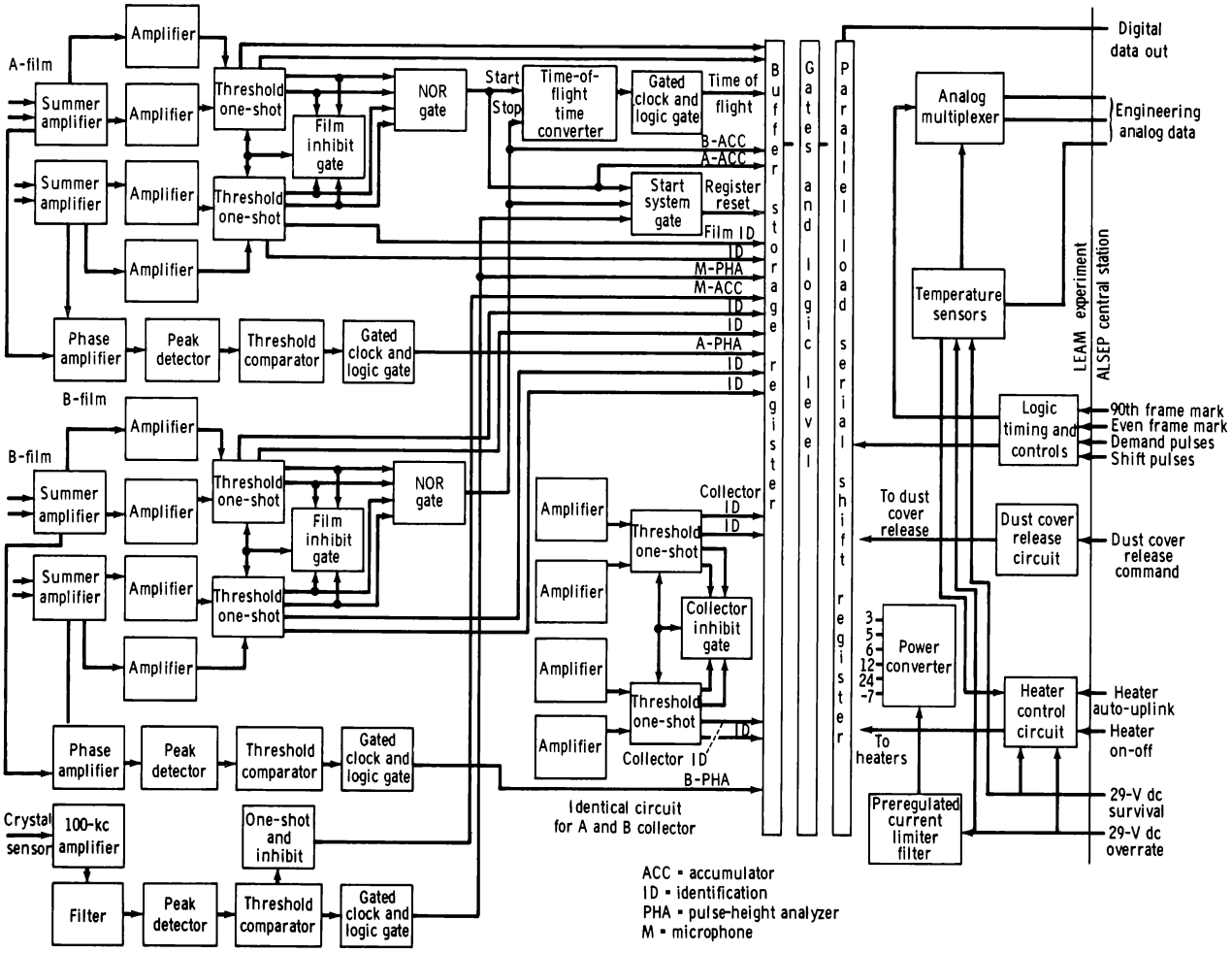

FIGURE 16-8.–Diagram of LEAM central electronics.

divides into two separate paths. In one path, it is amplified (voltage gain V_g equals 3.2 for each input), its pulse height is analyzed, and its amplitude is recorded in the storage register. In the other path, it is amplified (V_g = 5) and fed into a threshold one-shot. The output pulse performs three functions: its origin identification is impressed directly on the storage register; it passes through the logical NOR gate and initiates the time-of-flight measurement; and it is gated back to the threshold one-shot to inhibit any other A-film pulse until the measurement has been completed.

An inhibit signal to the other three films is necessary to avoid capacitative crosstalk for high-energy impact signals. The A-film pulse is pulse-height analyzed, and the results are stored in the register to await read-out.

Positive-going pulses from the B-film pass through a similar but separate electronic path, except that the B-film pulse is used to stop the time-of-flight clock. If no B-film pulse follows an A-film pulse, the time-of-flight register goes to the full (63 count) state and remains full until another event occurs.

Negative-going pulses from each of the grids (A and B) are amplified through separate units and identity (ID) registered as shown. For simplicity, only one set of collector amplifiers is shown in the lower center area of figure 16-8. Each film strip and each grid strip in both the front and the rear sensor arrays connects to its own separate amplifier system.

The output signal from the crystal sensor (microphone), as it responds to impacts, is a ringing sinusoidal wave that increases to a maxium and then decays. After amplification in a tuned amplifier, the peak signal amplitude is used to advance the microphone accumulate, to start the register reset

(read-out of register data), and to record the amplitude of the impulse imparted to the microphone sensor plate. The one-shot and the inhibit block shown in the microphone circuit inhibit further processing of subsequential microphone pulses until after the final pulse is placed in the storage register.

Pulses from the control microphone (not shown in the block diagram) follow a similar but separate electronic course, except that no pulse-height analysis is performed and the pulses do not trigger the register reset.

The sensors have been subjected to solar radiation simulators, including 3 MeV proton radiation and ultraviolet radiation. They showed no response or effects from radiation values as high as 100 solar constants.

DEPLOYMENT

The LEAM experiment was emplaced in the Taurus-Littrow area; its location is 43° east of north from the ALSEP central station at a distance of 7.5 m. As requested, the east sensor axis of the LEAM was directed 25° north of east to accommodate interstellar grains. The LEAM instrument was commanded "on" to operate for a period of 2 hr after deployment to verify proper performance. During this 2-hr period, two calibration commands were transmitted. The LEAM experiment responded with normal read-outs. It was commanded to the "off" mode until after lunar module (LM) ascent and detonation of the surface charges. The LEAM experiment was protected by two dust covers that were removed by ground command. One cover, designed to protect the thermal mirrors from dust contamination during LM ascent or from surface-charge detonations, was removed at a Sun angle of 130° (90° = lunar noon). A second cover, designed to protect the three sensor systems, was commanded "off" at 60 hr after lunar sunset of the first lunation. Because of the low data event rates anticipated (one event per day) for the LEAM experiment, it was essential to obtain a good measurement of the background noise or the extraneous pulse rate. Accordingly, the LEAM experiment output was recorded for periods of 60 hr of lunar day and 60 hr of lunar night with the sensor covers on. The covers were removed by a redundant squib system that was fired by command. A monitor signal indicated successful firing of both sets of squibs. In the case of the mirror-cover removal, a sudden decrease in the LEAM experiment temperatures verified successful removal.

However, in the case of the sensor covers, there was no noticeable change of temperature conditions inside the experiment following cover deployment. That fact and several subsequent observations of temperature excursions in the experiment have prompted an extensive study into the LEAM experiment temperature anomalies.

THE LEAM EXPERIMENT TEMPERATURES

Predicted temperatures for the LEAM experiment included a maximum of 146° F (336 K) at lunar noon and a minimum of −24° F (242 K) during lunar night. An automatic heater in the LEAM experiment turns on at 0° F (255 K) and off at 9° (261 K). The heater is designed to remain on continuously during lunar night and to keep the LEAM experiment temperatures above −24° F (242 K). In all cases, predicted temperatures were based on laboratory simulation studies. Actual temperatures for the LEAM experiment frame plotted against Sun angle (90° = lunar noon) during the first three lunations are shown in figure 16-9. The plot shows that the LEAM experiment is command "off" as its temperature approaches 167° (348 K), an arbitrarily acceptable operating temperature based on the highest operating temperature tested in the laboratory. This acceptable temperature will be increased to probably 212° F (378 K), pending the results of a total investigation of the temperature anomalies.

It is interesting to follow the temperature history of the LEAM experiment from the time of lunar emplacement. At a Sun angle of 130° during the first lunation, the mirror covers were removed, and the temperature decreased markedly. At a Sun angle of 162°, the LEAM experiment was commanded "on," in which mode it remained throughout the first lunar night. The thermostatically controlled heater cycled on and off approximately once per 6 hr. Temperature cycling was not unexpected while the sensor covers remained on. At a Sun angle of approximately 220° on the first lunar night, the sensor covers were commanded "off." No noticeable changes occurred in temperature cycling, although predictions indicated a temperature decrease and continuous heater operation.

At dawn of the second lunar day, the temperature

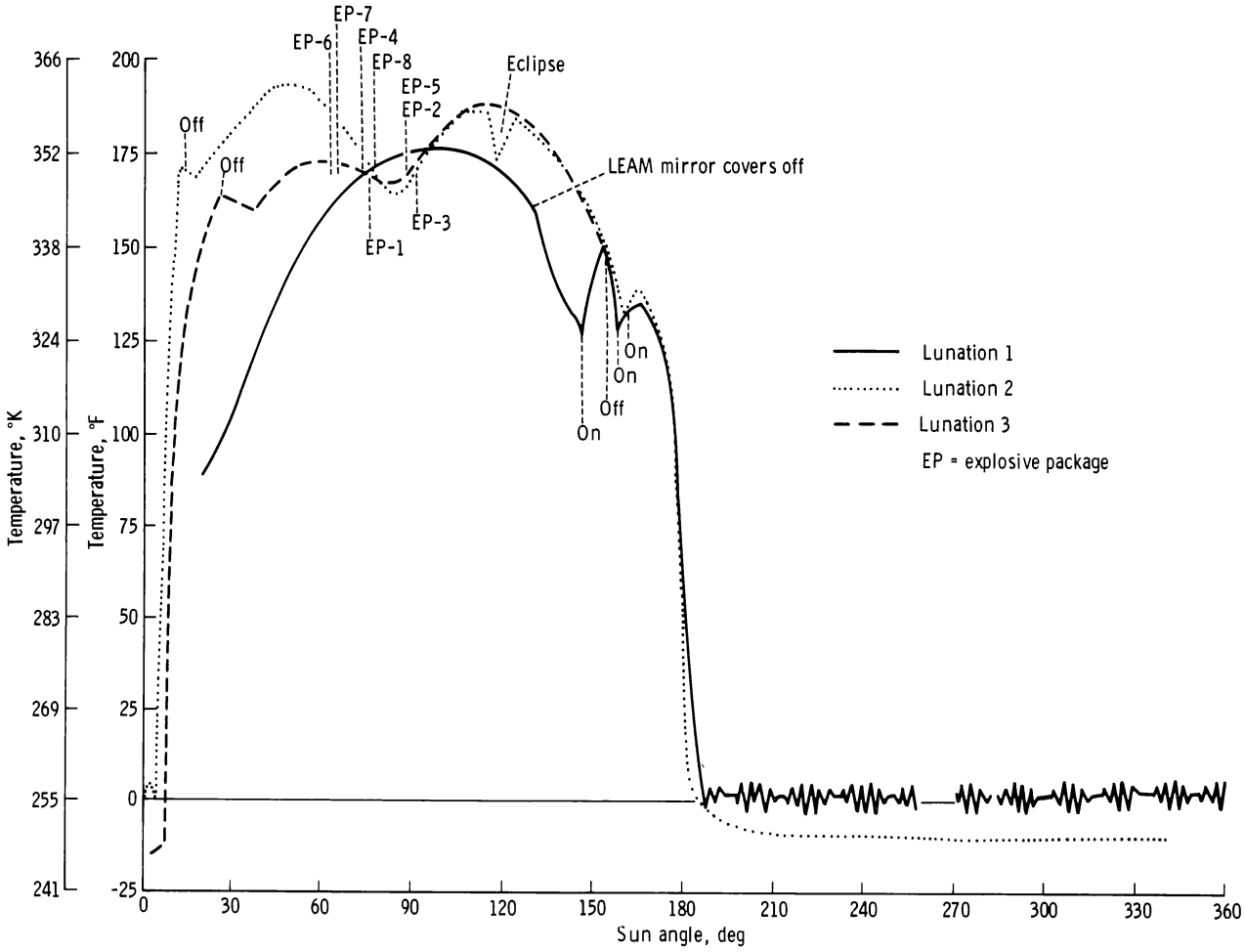

FIGURE 16-9.–The LEAM temperature history for three lunar days and two lunar nights.

rose rapidly to approximately 170° F (350 K) at a Sun angle of 15°, and the LEAM experiment was commanded "off" and remained in the "off" mode until a Sun angle of 160° when it was commanded "on." The LEAM experiment remained in this mode until dawn of the third lunar day. During the second lunar night, the registered temperatures were normal (as predicted), and the heater stayed on continuously. The strange behavior of the thermal sensor during the first lunar night compared to its normal behavior during the second lunar night indicated that the sensor covers had failed to deploy fully because of the extremely low temperatures. The temperature of the dust cover may have approached lunar surface temperatures. The sensor covers had presumably deployed sometime during dawn of the second lunation. The rapidly rising temperature at dawn of the second lunation is more difficult to explain.

A plausible explanation for the thermal anomalies is an accumulation of lunar dust on the sensor films. There is some evidence for electrostatic levitation of dust at the lunar sunset line (refs. 16-9 and 16-10). Positively charged dust particles would be attracted to and deposited on the negatively biased films; they would change the absorption/emission characteristics of a relatively large area of the LEAM experiment and cause heating. To preclude electrostatic dust accumulation at sunrise of the third lunation, the LEAM experiment was commanded "off" for a period of 75 min so that the experiment (and films) would maintain a similar potential to the lunar surface at the LEAM experiment site. Conceivably, the dust already deposited might be removed by electrostatic repulsion at sunrise. Interestingly, the third lunation temperatures were as much as 35° F (19.5 K) lower than the second lunation temperatures under identi-

cal conditions (Sun angle of 15°). A few degrees after lunar noon, the temperatures for the second and the third lunations were essentially identical.

It is interesting to consider further whether or not the LEAM experiment has, at least partially, verified electrostatic levitation of lunar dust. The LEAM experiment may eventually be manipulated to accommodate such studies; however, immediate plans are to operate it only at temperatures below 348 K to preserve it for the partial eclipse in June 1973. After the eclipse, the LEAM experiment will be operated continuously. Prelaunch thermal degradation analyses of the LEAM instrument show that it will operate at temperatures as high as 373 K with negligible degradation. (All electronic components for the LEAM experiment were qualified (tested) to a temperature of 257° F (398 K).) Meanwhile (preeclipse), the LEAM experiment will be operating during lunar nights, when conditions are ideal for the study of lunar ejecta, a major objective of the experiment.

RESULTS

No significant results are reported at the time of this report for the following reasons.

1. The anticipated event rate from the LEAM experiment is approximately one event per day (periods of and effects from meteoroid shower activity excepted).

2. It is now assumed that the sensor covers were not removed before dawn of the second lunation and probably were removed only hours before the experiment was commanded "off" during the lunar day. Accordingly, no significant real-time data were obtained during the 45-day support period.

3. All data tapes received to date contain only 150 hr of lunar day data and 620 hr of lunar night data with the LEAM experiment in the full operating mode (the experiment in the "on" mode and the sensor covers removed).

Meaningful results from the LEAM experiment can only be derived from a long-term statistical and correlative study between primary particle events and ejecta events. In view of the relatively short-term measurement of primary particles, it seems premature to extend results beyond making a statement that, with the exception of the high temperatures, the LEAM experiment is performing normally.

REFERENCES

16-1. Berg, O. E.; and Gerloff, U.: More Than Two Years of Micrometeorite Data From Two Pioneer Satellites. Space Research XI. Akademie-Verlag (Berlin), 1971, pp. 225-235.

16-2. Charters, A. C.: High-Speed Impact. Sci. Am., vol. 203, no. 4, Oct. 1960, pp. 128-140.

16-3. Shoemaker, Eugene; Moore, Henry; and Gault, Donald: Spray Ejected From the Lunar Surface by Meteoroid Impact. NASA TN D-1767, 1963.

16-4. Greenberg, J. M.: A Possible Inter-Relation Between Interstellar and Interplanetary Cosmic Dust. Space Research IX. North-Holland Publishing Co. (Amsterdam), 1969, pp. 111-115.

16-5. Gerloff, Uli; and Berg, Otto E.: The Orbits of 14 Elliptic and 6 Hyperbolic Micrometeoroids Derived From Pioneer-8 and -9 Measurements. Paper presented at the XVth COSPAR Meeting (Madrid, Spain), May 1972.

16-6. Rahe, J.; Donn, B.; and Wurm, K.: Atlas of Cometary Forms: Structures Near the Nucleus. NASA SP-198, 1969.

16-7. Kaiser, C. B.: The Thermal Emission of F Corona. Astrophys. J., vol. 159, Jan. 1970, pp. 77-92.

16-8. Berg, Otto E.; and Grun, Eberhard: Evidence of Hyperbolic Cosmic Dust Particles. Space Research XIII. Akademie-Verlag (Berlin), 1973.

16-9. O'Keefe, J. A.; Adams, J. B.; Gault, D. B.; Green, J.; et al.: Theory and Processes Relating to the Lunar Maria From the Surveyor Instruments. Surveyor 6 Mission Report. Part II: Science Results. Calif. Inst. Tech. Rept. JPL-TR-32-1262, Jan. 10, 1968, pp. 171-176.

16-10. Criswell, David R.: Lunar Dust Motion. Proceedings of the Third Lunar Science Conference, vol. 3, MIT Press (Cambridge, Mass.), Oct. 1972, pp. 2671-2680.